Electron paramagnetic resonance of Fe^{3+} ions in borate glass: computer simulations

1994 J. Phys.: Condens. Matter 6 9415

(http://iopscience.iop.org/0953-8984/6/44/020)

J. Phys.: Condens. Matter 6 (1994) 9415–9428. Printed in the UK

Electron paramagnetic resonance of Fe^{3+} ions in borate glass: computer simulations

El Mostapha Yahiaoui†, René Berger†, Yves Servant†, Janis Kliava‡, Leonid Čugunov§ and Andris Mednis§

† Centre de Physique Moléculaire Optique et Hertzienne, URA CNRS 283, Université Bordeaux I, F-33405 Talence Cédex, France

‡ Laboratoire de Cristallographie et de Physique Cristalline, URA CNRS 144, Université Bordeaux I, F-33405 Talence Cédex, France

§ Fizikas un Matemātikas Fakultāte, Latvijas Universitāte, Raiņa Bulvārī 19, LV-1098 Riga, Latvia

Received 17 March 1994

Abstract. Computer simulations of Fe^{3+} electron paramagnetic resonance spectra at X (9.5 GHz) and Q (34 GHz) bands in the alkali borate glass Li_2O–$2B_2O_3$ doped with Fe_2O_3 have been carried out using an approach based on the eigenfield method applied to the 'rhombic' spin Hamiltonian, which contains only the Zeeman and quadrupole fine-structure terms. In order to account for the structural disorder in the glass, two different distribution densities of fine-structure parameters D and E have been tried: a two-dimensional Gaussian function of D and $\lambda = |E/D|$, and the 'Czjzek function', analogous to the one used in Mössbauer-effect studies. In simulating the experimental spectra, care has been taken to fit not only to the most prominent features arising at $g_{ef} \simeq 4.3$ (at X and Q bands) and $g_{ef} \simeq 2.0$ (at Q band), but also to an obvious plateau of the derivative of the absorption, which extends down to the magnetic field corresponding to $g_{ef} \simeq 9.7$ (at both bands). As a result, the Czjzek function can be ruled out. The agreement between the experimental and computer-simulated spectra found with the Gaussian distribution density suggests the existence, besides orthorhombic symmetry sites (with $\lambda \simeq 1/3$), of a considerable number of Fe^{3+} sites with axial or feebly rhombic distortions ($\lambda \leqslant 0.08$). The relatively high mean value of the axial fine-structure parameter D is consistent with a highly distorted environment of Fe^{3+} ions in the glass.

1. Introduction

Oxide glasses doped with low concentrations of Fe^{3+} ions exhibit an X-band electron paramagnetic resonance (EPR) spectrum with a very prominent sharp peak ('singularity') with an effective g-factor $g_{ef} \simeq 4.3$, accompanied by a plateau ('shoulder') that extends to $g_{ef} \simeq 9.7$. In many cases, a peak at $g_{ef} \simeq 2.0$ is present as well. There has been a serious controversy in the literature concerning the adequate choice of the spin Hamiltonian to account for these resonances in glasses as well as in other disordered solids.

Beginning with the original works of Castner *et al* [1] and Wickman *et al* [2], most authors adopt the 'rhombic' spin Hamiltonian, in which all crystal-field terms other than the quadrupole fine structure are omitted:

$$\mathcal{H} = \beta g \mathcal{B} \cdot S + D[S_z^2 - \tfrac{1}{3}S(S+1) + \lambda(S_x^2 - S_y^2)]. \tag{1}$$

Here $S = 5/2$ and all symbols have their usual meaning. For simplicity, instead of the rhombic fine-structure parameter E, we prefer to use the ratio of rhombic and axial fine-structure parameters, $\lambda = |E/D|$. The principal axes x, y, z of (1) can always be chosen

0953-8984/94/449415+14$19.50

so that the λ values are within the limits $0 \leqslant \lambda \leqslant 1/3$, $\lambda = 0$ corresponding to purely axial symmetry of the environment of the paramagnetic ions and $\lambda = 1/3$ describing orthorhombic ('fully rhombic') symmetry, i.e. the maximal degree of rhombic distortion. (Note that in some earlier papers another choice of principal axes was made, e.g. see [1].) Following this description, several authors have calculated graphs of the resonance line positions (or effective g-factors) for different D and λ (or E) values and different orientations of the magnetic field B [3–8]. These graphs have been used to provide tentative estimates of D and λ values for Fe^{3+} in a number of non-crystalline matrices [7, 9], namely in borate glasses [10, 11].

An alternative approach to the interpretation of the $g_{ef} \simeq 4.3$ resonance has initially been put forward by Kedzie *et al* in a paper dealing with the Fe^{3+} ion in $CaWO_4$ crystals [12]. In this approach, one adopts a certain version of the spin Hamiltonian that includes quartic fine-structure terms assumed to possess *at least the same order of magnitude* as the quadrupole terms. From the latter, only the axial term is usually retained:

$$\begin{aligned}\mathcal{H} = \beta g \boldsymbol{B} \cdot \boldsymbol{S} &+ \tfrac{1}{6}a[S_x^4 + S_y^4 + S_z^4 - \tfrac{1}{5}S(S+1)(3S^2+3S-1)] \\ &+ \tfrac{1}{180}F[35S_z^4 - 30S(S+1)S_z^2 + 25S_z^2 - 6S(S+1) + 3S^2(S+1)^2] \\ &+ D[S_z^2 - \tfrac{1}{3}S(S+1)]. \end{aligned} \tag{2}$$

In spite of the fact that in the case of $CaWO_4$ this interpretation has later been disproved [13, 14], some authors attempt to apply it to Fe^{3+} and Mn^{2+} ions in glasses as well [15, 16]. The reader interested in this issue will find a relevant discussion in [17] and [18]. The main objection against the interpretation based on the spin Hamiltonian (2) is that, in fact, *in all cases* of $3d^5$ ions in crystalline hosts, where the spin Hamiltonian parameters can be unambiguously determined, the quartic fine-structure parameters turn out to be *small* in comparison with the Zeeman term (for X-band EPR spectra). This makes the latter interpretation rather questionable and explains why the bulk of the authors prefer the previous one, using the spin Hamiltonian (1). (Nevertheless, the approach stipulating the predominance of quartic fine-structure terms in the spin Hamiltonian has recently been resuscitated and the graphs of resonance magnetic fields have been calculated for this case [19].)

Because of the relative complexity of the formalism of computer treatment of the EPR spectra of disordered solids doped with ions possessing fine structure, only a few authors have attempted computer simulations of Fe^{3+} EPR spectra in glasses [17, 18, 20–23]. The X-band EPR spectra of Fe^{3+} in various glassy systems being very similar, one could have expected that a parametrization of these spectra by computer simulations would be straightforward. However, as surprising as this might seem, no reliable estimates of fine-structure parameters for this ion in glasses have yet been reported. This can be explained by the fact that, up to now, the majority of the authors turned their attention to fitting only to the most prominent feature centred at $g_{ef} \simeq 4.3$. Unfortunately, this feature can arise from a very large range of D and E values. (Note that this feature would also arise if one had used the spin Hamiltonian (2) to computer-simulate the EPR spectra of Fe^{3+}.) On the other hand, this is not the case with the low-field feature at $g_{ef} \simeq 9.7$, nor with the apparent plateau in the derivative-of-absorption spectra of Fe^{3+} extending from $g_{ef} \simeq 6$ to $g_{ef} \simeq 9$. Previously this part of the spectra has attracted little attention in the studies concerned with the computer simulation of EPR spectra. The resonance magnetic-field graphs given in [19] clearly demonstrate that the latter features disappear as the quartic spin Hamiltonian term depending on the parameter a (the 'cubic' fine structure) grows; see figures 1 and 5 in [19].

This provides one more piece of evidence for the inadequacy of the approach based on the spin Hamiltonian (2).

Thus, one may hope that, by attempting a computer fitting not only to the $g_{ef} \simeq 4.3$ peak but rather to the whole low-field portion of the Fe^{3+} EPR spectra in a glass on the basis of the spin Hamiltonian (1), the possible range of D and λ values could be substantially reduced.

The present paper reports on the computer simulations of the Fe^{3+} EPR spectra in a borate glass using a recently developed approach based on the eigenfield method [24]. The spin Hamiltonian (1) has been chosen on the basis of the reasoning presented above. The results obtained highlight the importance, for a reliable estimation of the spin Hamiltonian parameters in glassy hosts, of an accurate fitting to *all* features observed in the experimental spectra and not only to the most prominent ones.

2. Experiment: samples and spectra recording

A sample of formula $0.995(0.63B_2O_3–0.37Li_2O)0.005Fe_2O_3$ was prepared from a mixture of B_2O_3, Li_2O and Fe_2O_3 in suitable proportions, melted in a platinum crucible and quenched in air. The sample is feebly coloured. Its vitreous state has been tested by x-ray diffraction.

A Varian EPR spectrometer with a dual sample cavity was used to record the X-band spectra. The microwave frequency (9.516 GHz) was measured with a Hewlett–Packard frequency counter. The static magnetic field was measured by means of a nuclear fluxmeter associated with the same counter.

The Q-band spectra (33.94 GHz) were recorded with a Bruker spectrometer in the Laboratoire de Chimie de Coordination at the Université Paul Sabatier, Toulouse III (France).

The experimental room-temperature X- and Q-band EPR spectra are shown in figures 1(*a*) and (*b*). As one can see, these spectra are quite typical for the Fe^{3+} ions in oxide glasses. The most conspicuous feature in the X-band spectrum arises at $g_{ef} \simeq 4.3$; it is accompanied by a smooth plateau extending down to the 'shoulder' at $g_{ef} \simeq 9.7$. In the Q-band spectrum, besides these two features, an intense peak at $g_{ef} \simeq 2.0$ is observed.

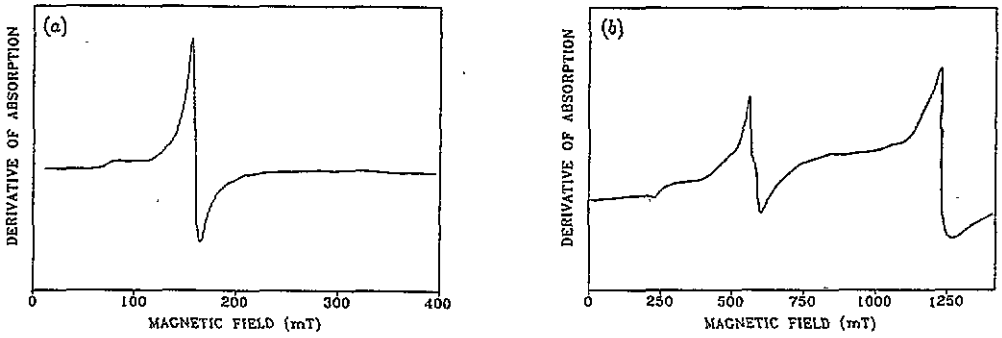

Figure 1. Experimental room-temperature EPR spectra of the glass $0.995(0.63B_2O_3–0.37Li_2O)0.005Fe_2O_3$ at (*a*) 9.516 GHz and (*b*) 33.94 GHz.

3. Principles of computer simulations

If one takes into account the distribution of the spin Hamiltonian parameters caused by the short-range disorder in the glass, as well as the complete orientational disorder of the paramagnetic ions, the EPR spectrum can be expressed as [17, 18]

$$\mathcal{P} = \int_{-\infty}^{\infty} \mathrm{d}D \int_{0}^{1/3} \mathrm{d}\lambda \int_{0}^{\pi} \mathrm{d}\theta \sin\theta \int_{0}^{2\pi} \mathrm{d}\phi \, P(D,\lambda) \left| \frac{\mathrm{d}B_{\mathrm{r}}(D,\lambda,\theta,\phi)}{\mathrm{d}\nu_{\mathrm{c}}} \right| \times W(D,\lambda,\theta,\phi) F(B - B_{\mathrm{r}}(D,\lambda,\theta,\phi), \Delta B). \tag{3}$$

Here $P(D,\lambda)$ is the joint distribution density of spin Hamiltonian parameters (the g-factor for Fe^{3+}, an S ion, only slightly deviates from the free-electron value $g = 2.0023$, and hence its distribution can be neglected); θ and ϕ are, respectively, the polar and azimuthal angles of the magnetic-field vector $\boldsymbol{B}$ in the x, y, z axes system; ν_{c} is the microwave frequency (a constant); W is the transition probability; and $F(B - B_{\mathrm{r}}, \Delta B)$ is the lineshape (usually taken as a Gaussian or a Lorentzian), with the linewidth ΔB determined by spin–lattice and spin–spin interactions and eventually including a broadening caused by smaller spin Hamiltonian terms neglected in (1). Thus, in order to computer-simulate the EPR spectrum in a glass, the resonance magnetic fields and transition probabilities must be calculated and the integration in (3) must be performed for a chosen functional form of $P(D,\lambda)$.

In typical cases of ions possessing Zeeman and fine-structure terms of the same order of magnitude, the procedure of computing a resonance magnetic field usually consists of repeated diagonalizations of the spin Hamiltonian matrix for different values of B, until the energy level separations match the energy quantum $h\nu_{\mathrm{c}}$; e.g. see [25]. In the present study, we have used a direct procedure based on the eigenfield method [26], recently adapted for the purpose of computer simulations of EPR spectra with distributed spin Hamiltonian parameters [24]. The resonance magnetic fields are computed by solving the generalized eigenvalue problem

$$\mathbf{A}_F Z = B \mathbf{A}_G Z \tag{4}$$

where

$$\mathbf{A}_F = h\nu \mathbf{1} \otimes \mathbf{1} - \mathbf{F} \otimes \mathbf{1} + \mathbf{1} \otimes \mathbf{F}^{+} \qquad \mathbf{A}_G = \mathbf{G} \otimes \mathbf{1} - \mathbf{1} \otimes \mathbf{G}^{+} \tag{5}$$

are Hermitian $n^2 \times n^2$ matrices ($n = 2S + 1$) obtained from the $n \times n$ spin Hamiltonian matrix $\mathbf{H}$, which, in turn, in most cases of interest can be written as

$$\mathbf{H} = \mathbf{F} + B\mathbf{G} \tag{6}$$

with $\mathbf{F}$ and $\mathbf{G}$ being, respectively, crystal-field and Zeeman operators. The eigenvectors of (4),

$$Z = u \otimes v^{*} \tag{7}$$

are direct products of two spin Hamiltonian matrix eigenvectors corresponding to the energy values ε and $\varepsilon - h\nu$:

$$\mathbf{H}u = \varepsilon u \qquad \mathbf{H}v = (\varepsilon - h\nu)v. \tag{8}$$

The relative weight of a given eigenvalue B_r is proportional to the square of the absolute value of the corresponding matrix element,

$$\mu_{vu} = \mu Z = \sum_{p=1}^{n^2} \mu_p Z_p \tag{9}$$

where μ_p are components of the electron magnetic moment operator expressed as a row vector. For Fe^{3+} ($S = 5/2$) $\mathbf{A}_F$ and $\mathbf{A}_G$ are 36×36 matrices.

The usual approach to the computation of EPR spectra with distributed spin Hamiltonian parameters consists of computing absorption spectra for fixed values of these parameters ('powder patterns') with a subsequent weighted summation according to the adopted distribution density; e.g. see [25]. Instead of this, we prefer to consider the entire EPR spectrum as a superposition of absorptions resulting from individual paramagnetic sites, each characterized by a distinct set of parameters D and λ and angles θ and ϕ. For each site, the values of D, λ, θ and ϕ are chosen at random, taking into account the distribution density of D and λ, as well as the isotropic distribution of orientations (the $\sin\theta$ factor in (3)). The generalized eigenfield problem (4) is solved for a chosen D, λ, θ and ϕ set, thus providing the resonance magnetic fields B_r^i and their intensities (relative weights) W_i. The whole magnetic-field range is subdivided into equal cells of width much narrower than the narrowest singularity in the experimental spectrum. For each site, numbers proportional to W_i are stored in the cells corresponding to the B_r^i values. As a result, a histogram of the absorption spectrum is formed.

At the next step, a convolution of this histogram is performed with a Gaussian or a Lorentzian derivative lineshape. This procedure has the triple objects of:

(i) transforming an absorption curve to a derivative of absorption for comparison with experiment;

(ii) smoothing the 'noise' in the calculated spectra; and

(ii) providing an additional broadening to account for distributions of spin Hamiltonian parameters omitted in (1), unresolved structures and relaxations.

4. Choice of the distribution density

The joint distribution density of spin Hamiltonian parameters in the EPR studies of glasses and other disordered solids most frequently is chosen in the form of a multidimensional Gaussian. For the spin Hamiltonian (1), neglecting a possible correlation between D and λ, one gets

$$P(D,\lambda) = \frac{C}{2\pi\Delta D\Delta\lambda}\exp\left(-\frac{(D-D_0)^2}{2\Delta D^2}\right)\exp\left(-\frac{(\lambda-\lambda_0)^2}{2\Delta\lambda^2}\right) \tag{10}$$

(note that all λ values outside the range of $0 \leqslant \lambda \leqslant 1/3$ must always be left out), where C is a normalization factor. A Gaussian distribution of parameters is usually related to the probability of a fluctuation, w (e.g. see [27]). For an isolated thermodynamic system, w is proportional to $\exp(\delta S/kT)$, where δS is the entropy variation due to the fluctuation and k is the Boltzmann constant. Since S is maximal at equilibrium, δS is a negative quadratic form of the thermodynamic variables. Therefore, w must be the Gaussian function of the latter. It is evident however that, if this reasoning can hold for such parameters as D and

E, having the dimension of energy (a thermodynamic parameter), it can hardly be applied to the dimensionless ratio $\lambda = |E/D|$. Nevertheless, (10) can be considered as a convenient approximation that permits one to evaluate the mean values and distribution widths of D and λ.

A somewhat different approach to the distribution density $P(D, \lambda)$ can be put forward on the basis of an analogy between the quadrupole fine-structure (QFS) parameters [28],

$$B_2^m = \left(\frac{4\pi}{5}\right)^{1/2} \langle r^2 \rangle \sum_k \frac{q_k}{R_k^3} (-1)^m Y_2^{-m}(\theta_k, \phi_k) \tag{11}$$

and the components of the electric-field-gradient (EFG) tensor [29],

$$V_2^m = \sum_k \frac{q_k}{R_k^3} Y_2^m(\theta_k, \phi_k). \tag{12}$$

In (11) and (12) q_k is the charge of the kth ligand, R_k, θ_k and ϕ_k are its radial, polar and azimuthal coordinates, Y_2^m are the second-order spherical harmonics and $\langle r^2 \rangle$ is the mean-square radius of the electron wavefunction. For the model of a random atomic arrangement, assuming a multidimensional Gaussian distribution of the EFG tensor components and taking into account the relation between the distribution of matrix elements and the distribution of eigenvalues, Czjzek *et al* [29] obtained

$$P(V_z, \eta) = \text{const} V_z^4 \eta \left(1 - \frac{\eta^2}{9}\right) \exp\left[-\frac{V_z^2}{2\sigma^2}\left(1 + \frac{\eta^2}{3}\right)\right] \tag{13}$$

where $\eta = 3\lambda = (V_x - V_y)/V_z$ and V_x, V_y and V_z are components of the *diagonalized* EFG tensor. If adapted to the QFS case (V_z, η and σ corresponding to $\frac{2}{3}D$, 3λ and $\frac{2}{3}\sigma'$, respectively), (13) can be written as

$$P(D, \lambda) = \text{const} D^4 \lambda (1 - \lambda^2) \exp\left(-\frac{D^2}{2(\sigma')^2}(1 + 3\lambda^2)\right). \tag{14}$$

It has ben shown by Le Caër *et al* [30] that the distribution (13) results from very general statistical considerations, namely, that (i) the solid is macroscopically isotropic and (ii) the EFG tensor components are distributed according to a multidimensional Gaussian law.

A number of modifications of the Czjzek distribution (13) have been proposed in order to account for the short-range ordering that persists to a certain extent in the vitreous state [30–33]. Namely, for the quadrupole splitting Δ, the following distribution density has been put forward [31]:

$$P(\Delta) = \text{const} \Delta^{d-1} \exp(-\Delta^2/2\sigma^2) \tag{15}$$

where

$$\Delta = \text{const} |V_z| (1 + \eta^2/3)^{1/2}$$

and $d \leqslant 5$ is the number of independent continuous random variables describing the manifold of site distortions. Adopting the distribution (15), one should replace D^4 by

D^{d-1} in the distribution (14) as well. However, it has been shown by Le Caër *et al* [30] that (15), in fact, does not actually correspond to a macroscopically isotropic system.

Another possible modification of (14) consists of reintroduction of *non-zero mean values* of the distributed fine-structure parameters, which are absent in the Czjzek function (13); e.g. see [33].

In the present study, the computer simulations of Fe^{3+} EPR spectra in borate glasses have been carried out assuming the Gaussian (10) or the Czjzek (14) distribution density $P(D, \lambda)$.

5. Results and discussion

The results of computer simulations of the EPR spectra are presented in figures 2 to 8. All simulations have been made with the Lorentzian derivative lineshape $F(B - B_r, \Delta B)$, see equation (3), which provides a better fit to the experimental EPR spectra. The peak-to-peak linewidth has been chosen as $\Delta B = 3.5$ mT at X band and $\Delta B = 8$ mT at Q band.

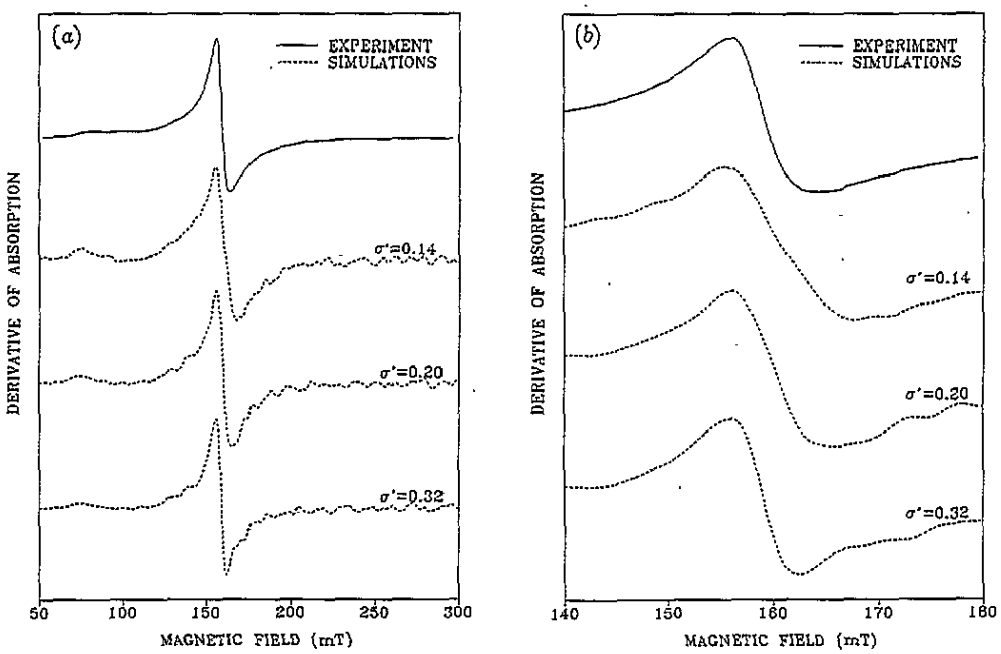

Figure 2. (*a*) Computer simulations of the experimental X-band EPR spectrum using the Czjzek distribution density (equation (14)) for different values of σ'. (*b*) The $g_{ef} \simeq 4.3$ feature on a greater scale.

First, we consider the X-band spectra simulations using the Czjzek distribution density (14); see figures 2(*a*) and (*b*). The only adjustable parameter in this case is the distribution width σ'. One can see from the computer-simulated spectra that in the chosen range of variation of σ' only the $g_{ef} \simeq 4.3$ and $g_{ef} \simeq 9.7$ features occur, in conformity with the experimental X-band spectrum. Within this range σ' mainly affects the width of the $g_{ef} \simeq 4.3$ feature and, as a consequence, the relative intensity of the $g_{ef} \simeq 9.7$ feature (the

maximum intensity in computer-simulated spectra being normalized to unity). The best fit to the $g_{ef} \simeq 4.3$ feature is attained in the vicinity of $\sigma' \simeq 0.20$. Meanwhile, as the whole range of σ' values corresponding to various widths of the $g_{ef} \simeq 4.3$ feature is scanned, the fit remains poor in the part of the spectra extending down to magnetic fields corresponding to $g_{ef} \simeq 9.7$. Indeed, instead of the smooth plateau apparent in this part of the experimental spectrum, an obvious hole shows in the computer-simulated ones. Thus, one can see that with the Czjzek function no satisfactory fit to the entire experimental Fe^{3+} EPR spectrum can be reached. Note that in the case of distribution (14) the most probable λ value (maximum of the marginal $P(\lambda)$ distribution) is

$$[\tfrac{1}{12}(15 - \sqrt{201})]^{1/2} \simeq 0.262.$$

This value is not far from the limiting one, $\lambda = 1/3$, corresponding to the 'fully rhombic' site symmetry. Therefore, the Czjzek function, in fact, describes a statistical ensemble of distorted sites, in which 'fully rhombic' distortions predominate.

So far, in the framework of analysis based on the spin Hamiltonian (1), it has been generally acknowledged that Fe^{3+} spectra in glasses with the most prominent feature at $g_{ef} \simeq 4.3$ arise from exactly this type of ensemble, in accordance with the theoretical results obtained using the perturbation theory. Indeed, the solution of the spin Hamiltonian (1) in the strong rhombic field case, $|D| = 3E \gg \beta g B$ [2, 17, 18, 34], results in the effective g-factors

$$g_x = g_y = g_z = \tfrac{30}{7} \simeq 4.3$$

for the middle Kramers' doublet, and

$$g_x = \tfrac{6}{7} \simeq 0.86 \qquad g_y = \tfrac{12}{7}(3 - \sqrt{7}) \simeq 0.61 \qquad g_z = \tfrac{12}{7}(3 + \sqrt{7}) \simeq 9.7$$

and

$$g_x = \tfrac{6}{7} \simeq 0.86 \qquad g_y = \tfrac{12}{7}(3 + \sqrt{7}) \simeq 9.7 \qquad g_z = \tfrac{12}{7}(3 - \sqrt{7}) \simeq 0.61$$

respectively, for the upper and lower Kramers' doublets (if $D > 0$). Thus, it can be concluded from the foregoing that such an ensemble obviously does not correspond to the real one.

Next, we proceed to the simulations obtained with the Gaussian function (10); see figures 3 to 8. In this case there are four adjustable parameters: D_0, ΔD, λ_0 and $\Delta\lambda$. The most general characteristics of computer-simulated spectra are as follows. As long as the distribution density for D values smaller than or comparable to $\beta g B$ is not negligible, the feature at $g_{ef} \simeq 2.0$ is always present. On the other hand, if D values greater than $\beta g B$ are most probable, the $g_{ef} \simeq 4.3$ feature prevails. Figure 3 illustrates the characteristic: the $g_{ef} \simeq 2.0$ feature becomes apparent if either the distribution of D is large enough to encompass the range of small D values (trace 2) or the mean D value, D_0, is sufficiently small (trace 3). As long as D_0 is greater than $\beta g B$ and/or the distribution of D is not too large, so as to avoid the range of small D values, the shape of the $g_{ef} \simeq 4.3$ feature is almost insensitive to the D_0 and ΔD values chosen; see figure 4. This makes a reliable estimation of these values from X-band spectra simulations extremely difficult.

In this context, the Q-band spectrum turns out to be of great utility, since it simultaneously shows both the $g_{ef} \simeq 4.3$ and $g_{ef} \simeq 2.0$ features; see figure 1. This fact

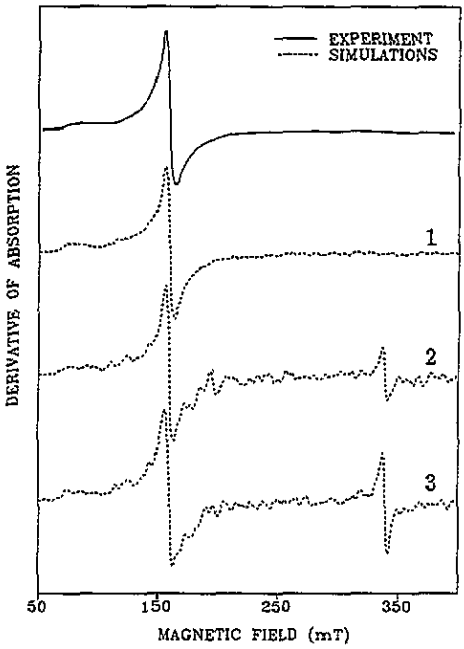

Figure 3. Computer simulations of the experimental X-band EPR spectrum using the Gaussian distribution density (equation (10)). The simulation parameters D_0, ΔD, λ_0 and $\Delta\lambda$ are, respectively: 0.6 cm^{-1}, 0.23 cm^{-1}, 0.04, 0.25 (trace 1); 0.6 cm^{-1}, 0.26 cm^{-1}, 0.02, 0.25 (trace 2); and 0.5 cm^{-1}, 0.23 cm^{-1}, 0.04, 0.25 (trace 3).

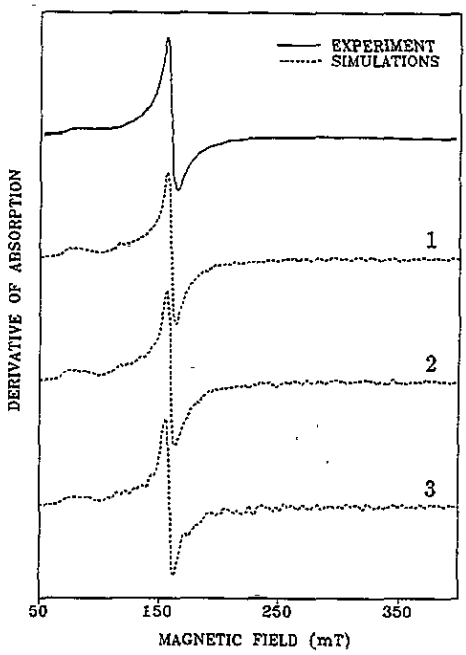

Figure 4. Computer simulations of the experimental X-band EPR spectrum using the Gaussian distribution density. The simulation parameters D_0, ΔD, λ_0 and $\Delta\lambda$ are, respectively: 0.6 cm^{-1}, 0.23 cm^{-1}, 0.04, 0.25 (trace 1); 0.5 cm^{-1}, 0.19 cm^{-1}, 0.04, 0.25 (trace 2); and 0.8 cm^{-1}, 0.28 cm^{-1}, 0.02, 0.25 (trace 3).

indicates that the D_0 value must not be too far from the microwave energy quantum, about 1.1 cm^{-1} at Q band. Therefore, the simulated Q-band spectra turn out to be much more sensitive to the D_0 and ΔD values in comparison to the X-band ones. As an example, two computer-simulated Q-band spectra are shown in figure 5. The upper one (trace 1) is in satisfactory agreement with the experimental spectrum in relative intensities of the $g_{ef} \simeq 4.3$ and $g_{ef} \simeq 2.0$ features; however, the peak-to-peak widths are much too narrow, thus indicating that a too high D_0 value has been chosen. The lower trace 2 provides a quite satisfactory fit to the experimental Q-band spectrum in both the relative intensities and peak-to-peak widths. The Q-band spectra simulations made so far are consistent with the D_0 and ΔD values within the following limits:

$$0.55 \leqslant D_0 \leqslant 0.85 \text{ cm}^{-1} \qquad 0.20 \leqslant \Delta D \leqslant 0.30 \text{ cm}^{-1}.$$

It is seen, however, that the noise level in the Q-band computer-simulated spectra remains high, in spite of the very important number of sites involved in the calculation (almost 180 000). Indeed, the calculated B_r values in this case are distributed in a very wide range (about 2400 mT). Therefore, more work seems to be necessary in order to specify further the D_0 and ΔD values.

On the other hand, the estimation of λ_0 and $\Delta\lambda$ can be made on the basis of X-band spectra simulations, in which case the range of calculated B_r values is much narrower and, consequently, the noise level is substantially lower, even for a smaller number of sites

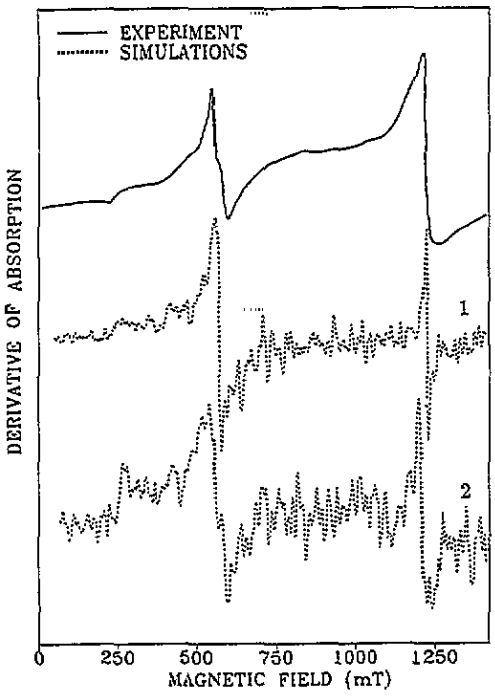

Figure 5. Computer simulations of the experimental Q-band EPR spectrum using the Gaussian distribution density. The simulation parameters D_0, ΔD, λ_0 and $\Delta\lambda$ are, respectively: 1.5 cm^{-1}, 0.62 cm^{-1}, 0.06, 0.18 (trace 1); and 0.6 cm^{-1}, 0.23 cm^{-1}, 0.04, 0.25 (trace 2).

involved (see figures 3, 4, 6, 7 and 8). The X-band spectra computed with the characteristics of D values distribution quoted above and with λ values distributed in the range from about 0.08 to 1/3 always show the sharp feature at $g_{ef} \simeq 4.3$ and the 'shoulder' at $g_{ef} \simeq 9.7$. Nevertheless, all simulations carried out with λ_0 ranging from 0.08 to 1/3 fail to provide a satisfactory fit to the part of the EPR spectrum between $g_{ef} \simeq 9.7$ and $g_{ef} \simeq 4.3$. Indeed, all these simulations (see two examples with $\lambda_0 = 0.18$ and 0.10 in figure 6, traces 1 and 2) inevitably show the same type of hole as the simulations using the Czjzek function. Thus, in order to be able to 'fill up' this hole, one is bound to reconsider the statistical ensemble of site distortions contributing to the experimental EPR spectra. Computer simulations made with different non-distributed values of $\lambda \leqslant 0.08$ (not shown here) demonstrate a net shift of the $g_{ef} \simeq 9.7$ feature towards $g_{ef} \simeq 6.0$ as λ approaches zero. This behaviour can also be established by inspecting appropriate graphs in the paper by Aasa [5], as well as on the basis of the perturbation theory analysis. Indeed, it is well known (e.g. see [1]) that, for $|D| \gg \beta g B$ and $\lambda = 0$ (axially symmetric sites), the spin Hamiltonian (1) provides three Kramers' doublets, $|\pm 5/2\rangle$, $|\pm 3/2\rangle$ and $|\pm 1/2\rangle$, only within the latter one of which are the EPR transitions allowed. The corresponding g-factors are [1]

$$g_x = g_y = g_\perp = 6.0 \qquad g_z = g_\parallel = 2.0.$$

One can conclude that, in order to provide an additional absorption in the range of effective g-values corresponding to the plateau in the derivative-of-absorption spectrum, the statistical ensemble of Fe^{3+} sites must comprise a considerable portion of sites with axial and feebly

rhombic ($\lambda \ll 1/3$) distortions. Indeed, the computer simulations carried out with the Gaussian distribution density (10) and $\lambda_0 \leqslant 0.08$ show a much better agreement with the experiments in the range $5 \leqslant g_{ef} \leqslant 10$; see trace 3 in figure 6, as well as figure 7.

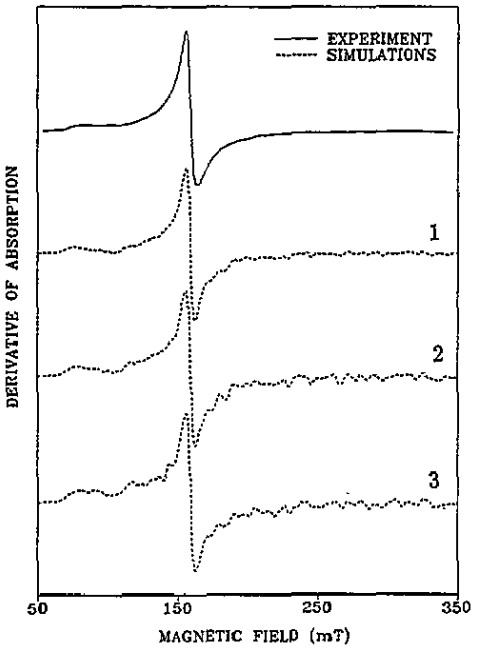

Figure 6. Computer simulations of the experimental X-band EPR spectrum using the Gaussian distribution density. The simulation parameters D_0, ΔD and $\Delta\lambda$ are, respectively, 0.8 cm^{-1}, 0.28 cm^{-1} and 0.18 for all three computed spectra. The parameter λ_0 is 0.18 (trace 1), 0.10 (trace 2) and 0.05 (trace 3).

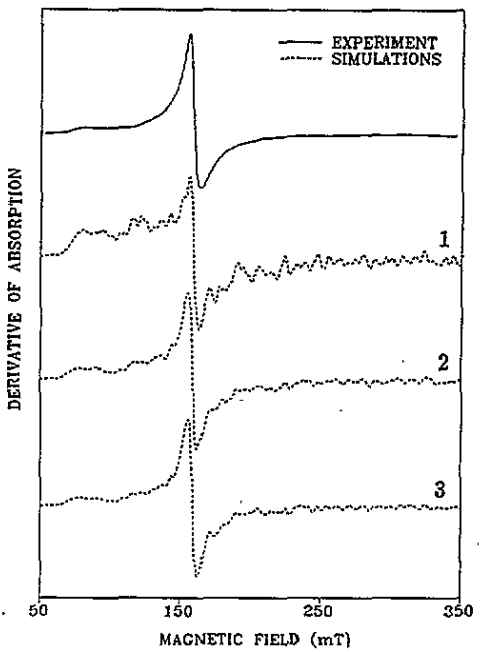

Figure 7. Computer simulations of the experimental X-band EPR spectrum using the Gaussian distribution density. The simulation parameters D_0 and ΔD are, respectively, 0.8 cm^{-1} and 0.28 cm^{-1} for all three computed spectra. The parameters λ_0 and $\Delta\lambda$ are, respectively: 0.04 and 0.14 (trace 1); 0.04 and 0.20 (trace 2); and 0.03 and 0.25 (trace 3).

In this context, it seems pertinent to recall to the reader's attention that Castner *et al* [1] assumed from structural inferences a very important part (about 2/3) of Fe^{3+} ions in silicate glasses to be in axially symmetric sites. They claimed, however, not to observe these sites in the EPR spectra. Still, an inspection of figure 1 in their paper [1] suggests the presence of approximately the same portion of Fe^{3+} ions in axial sites in the silicate glasses as in the borate one (cf with figure 1(*a*) of the present paper).

Furthermore, a good computer fit to the relative intensities of the 'shoulder' at $g_{ef} \simeq 9.7$ and the sharp feature at $g_{ef} \simeq 4.3$ in the experimental X-band EPR spectrum can only be reached if one assumes a sufficiently wide distribution of λ, which encompasses λ values tending towards 1/3, as well (see figure 8(*a*)). The most satisfactory computer-simulated spectra are obtained for λ_0 and $\Delta\lambda$ within the following limits:

$$0.025 \leqslant \lambda_0 \leqslant 0.055 \qquad 0.20 \leqslant \Delta\lambda \leqslant 0.27$$

see figures 8(*a*) and (*b*), traces 1 and 2. (We remind the reader that the λ values are always confined between 0 and 1/3; consequently, values outside this range must be excluded from

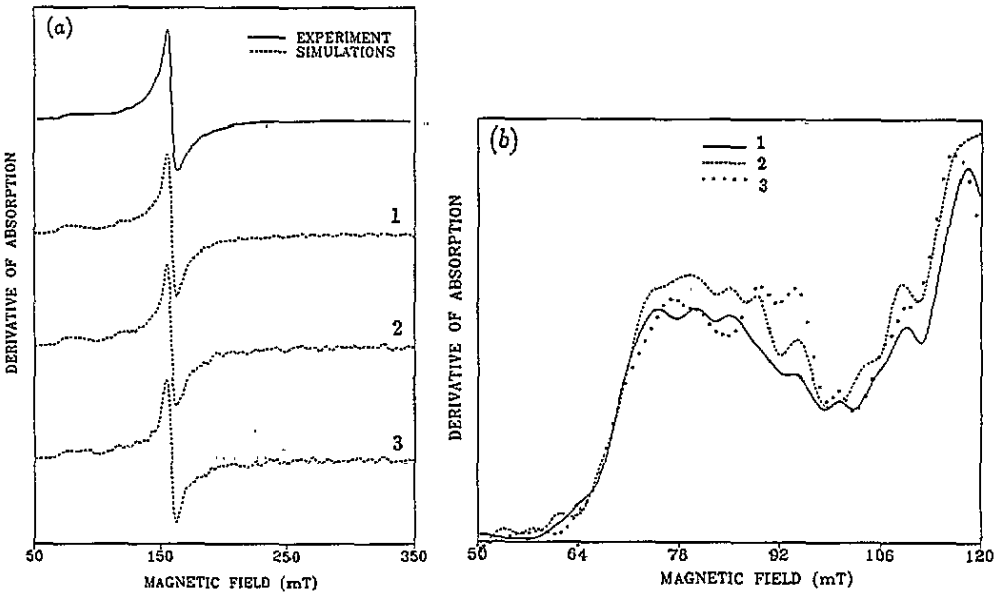

Figure 8. (*a*) Computer simulations of the experimental X-band EPR spectrum using the Gaussian distribution density. The simulation parameter $\Delta\lambda$ is 0.25 for all three computed spectra. The parameters D_0, ΔD and λ_0 are, respectively: 0.6 cm^{-1}, 0.23 cm^{-1} and 0.04 (trace 1); 0.6 cm^{-1}, 0.23 cm^{-1} and 0.02 (trace 2); and 0.8 cm^{-1}, 0.28 cm^{-1} and 0 (trace 3). (*b*) The low-field part of the simulated spectra on a greater scale.

consideration.) Note that λ_0 values less than 0.02, while preserving the plateau in the low-magnetic-field range, produce too much intensity in the $g_{ef} \simeq 6.0$ range; see figure 8(*b*), traces 2 and 3.

As far as the best-fit parameters of the distribution density of spin Hamiltonian parameters found in this study are concerned, it is interesting to note that relatively high values of D_0, previously reported for Fe^{3+} in a series of alkaline-earth phosphate glasses [17, 18], are close to that found for the borate glass. These values imply a highly distorted environment for Fe^{3+} ions in oxide glasses. On the other hand, the broad distribution of λ values found for the borate glass seems to be in contrast with relatively narrow distributions of the fine-structure parameter E in phosphate glasses [17, 18]. This discrepancy may be due to different forms of the distribution density of fine-structure parameters used in computer simulations in the two cases.

Finally, it should be noted that, as a close inspection of figure 8(*b*) reveals, in spite of the visibly improved fit to the experimental Fe^{3+} EPR spectra for low λ_0 values, a certain disagreement persists, which cannot be removed within the framework of the distribution density (10). In this connection, it would certainly be interesting to attempt computer simulations of the Fe^{3+} EPR spectra in glasses using distribution densities other than (10) and (14). These simulations are at present in progress. Nevertheless, already at this stage one can argue that the relatively high probability of small λ values, as inferred from the above analysis, rules out all distribution densities that contain λ (respectively, η) as a factor, that is, not only the Czjzek function, but also those put forward in [29–33]. If this proved true, there should exist a certain difference between the functional forms of distribution densities of EFG and QFS in glass.

6. Conclusions

The experimental EPR spectra of Fe^{3+} ions in oxide (borate) glass are well described by the 'rhombic' spin Hamiltonian that contains only the Zeeman and quadrupole fine-structure terms. The fine-structure parameter distribution function analogous to that used by Czjzek *et al* [29] in Mössbauer-effect studies cannot satisfactorily account for the spectral shape of Fe^{3+} in borate glass. The two-dimensional Gaussian function certainly provides a much better approach to the actual distribution density of the fine-structure parameters. The best-fit fine-structure parameter values obtained for the borate glass imply that:

(i) the environment of Fe^{3+} ions is highly distorted; and

(ii) in contrast to the generally acknowledged concept, according to which the predominance of the $g_{ef} \simeq 4.3$ feature in the EPR spectra of glasses is considered as a manifestation of orthorhombic distortions ($\lambda_0 \simeq 1/3$), an important part of Fe^{3+} ions in borate glass are subject to axial or feebly rhombic distortions from cubic symmetry ($\lambda \leqslant 0.08$).

As far as very similar EPR spectral shapes of Fe^{3+} ions are observed in borate, phosphate and silicate glasses [17, 18], it seems that analogous conclusions can be applied to other vitreous oxides as well.

Acknowledgments

The authors are indebted to Professor A Levasseur of the Laboratoire de Chimie du Solide of the CNRS and ENSCPB, Université Bordeaux I, for preparing the glass sample and for valuable discussions. Thanks are due to Dr A Mari of the Laboratoire de Chimie de Coordination, Université Paul Sabatier, Toulouse III, for recording the Q-band spectra. The experimental cooperation of Dr P Béziade is gratefully acknowledged.

References

[1] Castner T Jr, Newell G S, Holton W C and Slichter C P 1960 *J. Chem. Phys.* **32** 668
[2] Wickman H H, Klein M P and Shirley D A 1963 *J. Chem. Phys.* **42** 2113
[3] Griscom D L and Griscom R E 1967 *J. Chem. Phys.* **47** 2711
[4] Dowsing R D and Gibson J F 1969 *J. Chem. Phys.* **50** 294
[5] Aasa R 1970 *J. Chem. Phys.* **52** 3919
[6] Nicklin R C, Farach H A and Poole C P Jr 1976 *J. Chem. Phys.* **65** 2998
[7] Sperlich G and Urban P 1974 *Phys. Status Solidi* b **61** 475
[8] Brodbeck C M 1980 *J. Non-Cryst. Solids* **40** 305
[9] Friebele E J, Wilson L K, Dozier A W and Kinser D L 1971 *Phys. Status Solidi* b **45** 232
[10] Loveridge D and Parke S 1971 *Phys. Chem. Glasses* **12** 19
[11] Dance J M, Darnaudery J P, Baudry H and Monneraye M 1981 *Solid State Commun.* **39** 199
[12] Kedzie R W, Lyons D H and Kestigian M 1965 *Phys. Rev.* **138** A918
[13] Golding R M, Kestigian M and Tennant C W 1978 *J. Phys. C: Solid State Phys.* **11** 5041
[14] McGavin D G and Tennant W C 1985 *J. Magn. Reson.* **61** 321
[15] Chepeleva I V 1972 *Dokl. Akad. Nauk SSSR* **202** 1042
[16] Zhilinskaya E A and Lazukin V N 1982 *J. Non-Cryst. Solids* **50** 163
[17] Kliava J 1986 *Phys. Status Solidi* b **134** 411
[18] Kliava J 1988 *EPR Spectroscopy of Disordered Solids* (EPR spektroskopia neuporiadochennyh tverdyh tel) (Riga: Zinàtne) (in Russian)
[19] Černý V 1992 *Phil. Mag.* B **65** 401
[20] Sweeney W V, Coucouvanis D and Coffman R E 1973 *J. Chem. Phys.* **59** 369

[21] Coffman R E 1975 *J. Phys. Chem.* **79** 1129
[22] Scullane M I, White L K and Chasteen N D 1982 *J. Magn. Reson.* **47** 383
[23] McGavin D G and Tennant W C 1985 *J. Magn. Reson.* **62** 357
[24] Čugunov L, Mednis A and Kliava J 1994 *J. Magn. Reson.* A **106** 153
[25] Brodbeck C M and Iton L E 1985 *J. Chem. Phys.* **83** 4285
[26] Belford G G, Belford R L and Burkhalter J F 1973 *J. Magn. Reson.* **11** 251
[27] Hansen J P and McDonald I R 1976 *Theory of Simple Liquids* (New York: Academic)
[28] Abragam A and Bleaney B 1970 *Electron Paramagnetic Resonance of Transition Ions* (Oxford: Clarendon)
[29] Czjzek G, Fink J, Götz F, Schmidt H, Coey J M D, Rebouillat J-P and Liénard A 1981 *Phys. Rev.* B **23** 2513
[30] Le Caër G, Dubois J M and Brand R A 1984 *Amorphous Metals and Nonequilibrium Processing* ed M von Allmen (Les Ulis, Fr.: Les Editions de Physique) p 243
[31] Czjzek G 1982 *Phys. Rev.* B **25** 4908
[32] Le Caër G, Brand R A and Dehghan K 1985 *J. Physique Coll.* **46** (C8) 169
[33] Maurer M 1986 *Phys. Rev.* B **34** 8996
[34] Nicklin R C, Poole C P Jr and Farach H A 1973 *J. Chem. Phys.* **53** 2579